International Journal of Current Engineering and Technology
E-ISSN 2277 – 4106, P-ISSN 2347 – 5161

Available at http://inpressco.com/category/ijcet

Research Article

Design of Magnetorheological Brake using Parabolic Shaped Rotating Disc

Chiranjit Sarkar†* and Harish Hirani‡

†Mechanical Engineering Department, Delhi Technological University, Shahbad Daluatpur, Bawana Road, Delhi – 110042, India
‡Mechanical Engineering Department, Indian Institute of Technology Delhi, Hauz Khas, New Delhi – 110016, India

Accepted 16 March 2015, Available online 18 March 2015, **Vol.5, No.2 (April 2015)**

Abstract

The aim of this paper is to enhance the braking torque of a magnetorheological brake (MRB) system. The proposed brake system consists of rotary disc with wave form boundary immersed in a MR fluid and enclosed in an electromagnet. The yield stress of the fluid varies as a function of magnetic field created by electric current passing through the electromagnet. The instantaneous increase in yield stress of fluid significantly increases the friction on the surfaces of rotating disks; thus generating a retarding braking torque. Due to the waveform boundary, a wedge shape is formed between the outer fixed casing and the disc. This wedge shape provides the extra resisting force to stop the rotation of the disc due to the shear stress of the MR fluid changed with the influence of the applied magnetic field. In the present study, the Bingham model has been used to estimate the braking torque exercised by MR brake. A parametric study considering various configurations of rotating disk and MR gap has been presented. Parabolic profile MR brake shows the large braking torque compared to circular profile of disc.

Keywords: *MR fluid, MR brake, Waveform boundary disc*

1. Introduction

Magnetorhelogical (MR) suspensions are known for dramatic change in their apparent viscosity. Due to their variable viscosity, MR fluids are used in engineering applications requiring controllable dynamic performance. One such application is magnetorheological brake in which MR fluid is treated as a brake lining material. This material does not wear-away and provides desirable friction resistance by just controlling the magnetic field passing through it. As MR brake involves electromagnetism and magnetizable friction material, this system can be named as "electromagnetic brake" (Gupta and Hirani, 2011).

A typical MR fluid consists of 20-40 volume percentage of pure-iron (purity > 99%) particles (size: Ø3-10 micrometers), suspended in a carrier liquid such as mineral oil, synthetic oil, water or glycol. A variety of proprietary additives to avoid gravitational settling, to elude wear and to promote particle suspension, are added to MR fluids. To model the behavior of MR fluids, the Bingham plastic model (Ginder and Davis, 1994) is used. MR fluids exhibit maximum yield strengths of 50-100 kPa for applied magnetic fields of 150-250 kA/m. The performance of MR-based devices is relatively insensitive to temperature over a broad temperature range (Ginder and Davis, 1994).

*Corresponding author: **Chiranjit Sarkar**

The design of MR brake starts with the maximum shear strength, τ_{max}, achievable by the available MR fluid. The control on the shear stress (between zero to τ_{max}) of MR fluid is achieved by regulating the magnitude and direction of the magnetic field. The field density is a function of permeability and saturation of materials through which magnetic field passes, brake geometry, number of turns in electromagnetic coil, and current supplied to electromagnetic coil (Sarkar and Hirani, 2015), (Sarkar and Hirani, 2013), (Sukhwani, *et al*, 2009), (Sukhwani and Hirani, 2008), (Sukhwani and Hirani, 2008), (Sukhwani, *et al*, 2008), (Hirani and Manjunatha, 2007), (Sukhwani, *et al*, 2007),(Sukhwani and Hirani, 2007), (Sukhwani, *et al*, 2006). Unfortunately, MR fluids do not show linear increment in shear strength with increase in applied magnetic field, and finally shear strength gets saturated. Therefore in the present study, the non-linear behavior of shear strength and saturation limits to estimate the braking torque exercised by MR brake have been incorporated.

2. Mathematical Modeling of MR brake using conventional disc

The braking action on MR brake is achieved due to the change in shear stress of the MR fluid in the presence of the magnetic field. The shear stress of MR fluid is modelled as the Bingham model as shown in Eq. (1)

$$\tau = \tau_o + \eta \frac{du}{dy} \quad (1)$$

Where, $\tau_o = \alpha\left(\frac{NI}{2h}\right)^{\beta}$ depends on the applied magnetic field, α and β are the constants depend on the MR fluid properties.

Figure 1 shows the schematic of MR brake. Low carbon steel is selected for the casing as well as the disc material because to magnetize the MR fluid the material of the casing and the disc should be magnetic, low carbon is the magnetic material and it is easily available. Stainless steel is selected for the shaft material; because the MR fluid at the seal should not be magnetized otherwise the seal will break. The nitrile rubber seal is good option at the low as well as at high speed.

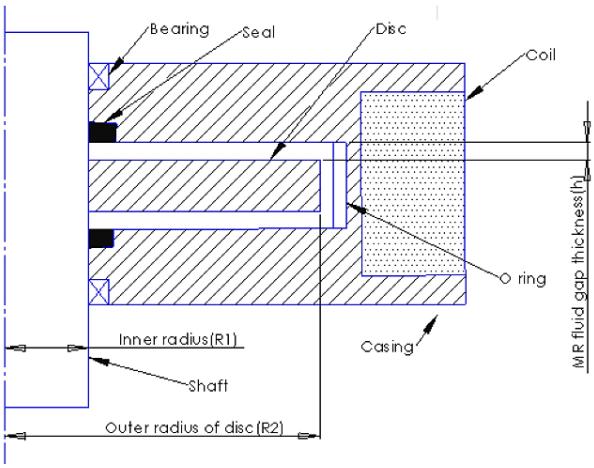

Fig.1 Schematic of MR brake with conventional disc

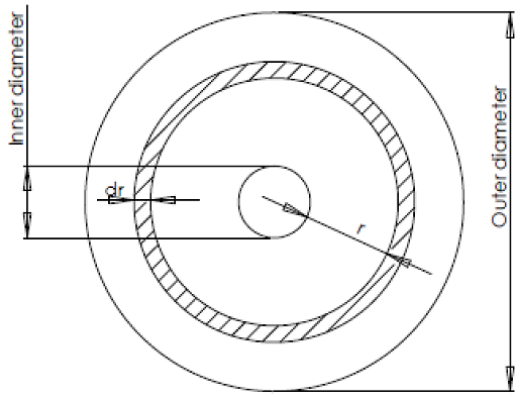

Fig.2 Geometry of conventional disc

The area of the element shown in the Figure 2 is shown in Eq. (2).

$$da = 2\pi r dr \quad (2)$$

The resisting force on the disc surface will act due to the shear stress of the MR fluid. The force acting on the element is

$$dF = \tau(2\pi r dr) \quad (3)$$

$$dF = \left(\tau_o + \eta \frac{du}{dy}\right)(2\pi r dr) \quad (4)$$

For MRF 241ES, $\alpha = 2.78 \times 10^{-4}\left(m/A\right)^{1.5}$ and β = 1.5.

The braking torque acting on the disc is

$$dT = \int_{R1}^{R2} h\left(\tau_o + \eta \frac{du}{dy}\right) 2\pi r dr \quad (5)$$

Therefore, the total braking torque with two working surfaces is given as

$$T = 2\pi h \tau_o \left(R_2^2 - R_1^2\right) + \frac{4\pi\eta\omega}{3h}\left(R_2^3 - R_1^3\right) \quad (6)$$

3. Mathematical Modeling of MR brake using Waveform boundary disc

In finite element analysis for multi-plate MR brake (Sarkar and Hirani, 2015) estimated brake torque was approximately 300 Nm, which is lesser than the required braking torque for automotive applications. In order to enhance the braking torque, comprehensive study of MR brake is required. One way is to explore additional modes, i.e. compression, squeeze, of MR fluids. To implement compression and squeeze modes of MR fluid, there is a need to change in design of rotating disc and brake assembly. Nam and Ahn (2009) introduced waveform shaped disc in MR brake. Two such wave-formed discs, as shown in Figure 3 and Figure 4, have been explored in the present manuscript.

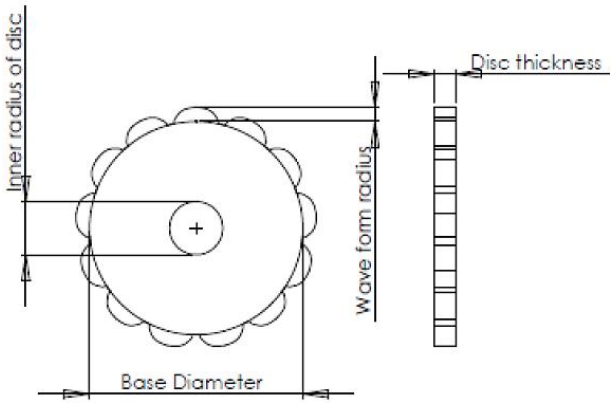

Fig.3 Disc with parabolic waveform

Due to the waveform boundary, a wedge shape is formed between the outer fixed casing and the disc. This wedge shape provides the extra resisting force to stop the rotation of the disc due to the shear stress of the MR fluid is changed with the influence of the applied magnetic field. The wedge shape and the fixed casing are shown in Figure 5.

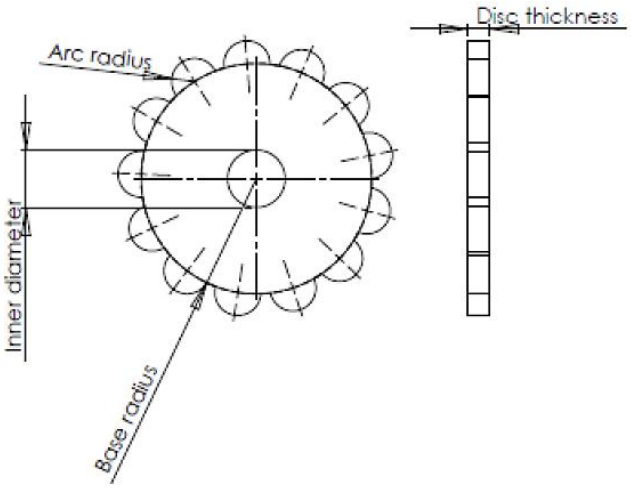

Fig.4 Disc with circular waveform

The friction force generated is given in Eq. (7).

$$F = \int_0^t \int_0^l \tau dx dz \tag{7}$$

t = thickness of the disc

l = contact length of the wave form.

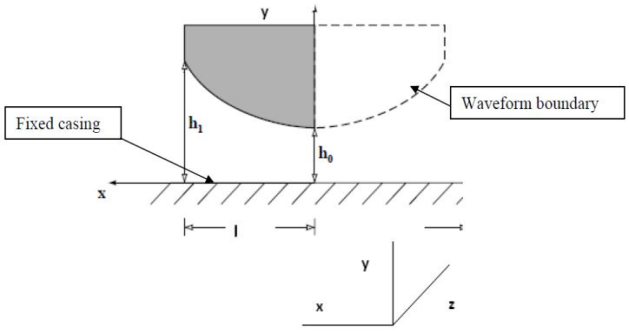

Fig.5 Schematic diagram of parabolic wedge shape

The braking action in MR brake is achieved due to change in shear stress of MR fluid in the presence of the magnetic field. The shear stress of MR fluid is modeled as the Bingham model as in Eq. (8).

$$\tau = \tau_0 + \eta \frac{du}{dy} \tag{8}$$

So the frictional force after putting the value of shear stress from Eq. (8).

$$F = \int_0^t \int_0^l \left(\tau_0 + \eta \frac{du}{dy}\right) dx dz \tag{9}$$

So the resistance force generated due to the first term of the equation.

$$F_1 = \tau_0 l t \tag{10}$$

Where, $\tau_0 = \alpha \left(\frac{NI}{2h}\right)^{\beta}$

Resistance force due to the viscosity of MR fluid is

$$F_{vis} = \int_0^t \int_0^l \eta \frac{du}{dy} dx dz \tag{11}$$

$\frac{du}{dy}$, obtained from the differentiating the velocity equation and given as

$$u = \frac{1}{2\eta}\frac{\partial p}{\partial x} y(y-h) + \frac{(y-h)U}{h} \tag{12}$$

U is the constant velocity of the disc. Then from Eq. (12)

$$\frac{du}{dy} = \frac{1}{2\eta}\frac{\partial p}{\partial x}(2y-h) - \frac{U}{h} \tag{13}$$

Then the viscous force

$$F_{vis} = \int_0^t \int_0^l \frac{1}{2\eta}\frac{\partial p}{\partial x}(2y-h) dx dz - \int_0^t \int_0^l \frac{U}{h} dx dz \tag{14}$$

The friction force will be maximum at the lower surface (y = 0) so the maximum force

$$F_{vis} = \int_0^t \int_0^l \frac{1}{2\eta}\frac{\partial p}{\partial x}(-h) dx dz - \int_0^t \int_0^l \frac{U}{h} dx dz \tag{15}$$

The film geometry for the parabolic profile is

$$h = h_0 + (h_1 - h_0)\left(1 + \frac{x}{l}\right)^2 \tag{16}$$

The film geometry for the spherical wedge profile is

$$h = h_1 - \sqrt{(h_1 - h_0)^2 - x^2} \tag{17}$$

The resisting torque has been calculated for the parabolic profile and for the circular profile by putting the value of h from the Eq. (16) into the Eq. (15) after integrating Eq. (15) and applying the boundary condition

p = 0 at x = 0 and p =0 at x = 1.

The integration of first term of Eq. (15) is

$$l_1 = \frac{h_1 - h_0}{l}(1+l) p t l$$

$$l_1 = \frac{h_1 - h_0}{l}(1+l) w$$

And $w = \frac{6U\eta l t^2}{k^2 {h_0}^2}\left(-\ln(K+1) + \frac{2K}{K+2}\right)$

Where $K = (h_1 - h_0)/h_1$ then

$$l_1 = \frac{(h_1 - h_0)}{l}(1+l)\frac{6U\eta l t^2}{k^2 {h_0}^2}\left(-\ln(K+1) + \frac{2K}{K+2}\right) \tag{18}$$

The integration of the second term of the equation will be.

$$l_2 = \frac{tU\eta h_0}{\sqrt{K}}[tan^{-1}R] \quad (19)$$

Where $R = \left(1 + \frac{l}{t}\right)\sqrt{K}$

The total resisting force due to the parabolic profile

$$F_{total} = \left(l_1 + l_2 + \alpha(NI/2h)^{\beta} lt\right) \times no\ .ofarc \quad (20)$$

Braking torque from the frictional resistance force due to the waveform boundary is

$$T_{waveform} = F_{total} \times R_2$$

Total braking torque acting on the rotating disc will be the combination of the braking torque due to the waveform boundary and the braking torque due to the conventional disc (T).

Total braking torque

$$T_{total} = T_{waveform} + T \quad (21)$$

Total braking for the parabolic waveform is larger than the circular waveform, the theoretical results discussed below.

3. Results and Discussions

Considering the values of τ_o (= 56 kPa), h (= 1 mm), R_1 (= 50 mm) and ω (= 30 rad/s), the braking torque of MR brake has been estimated using Eq. (6) and plotted in Figure 6.

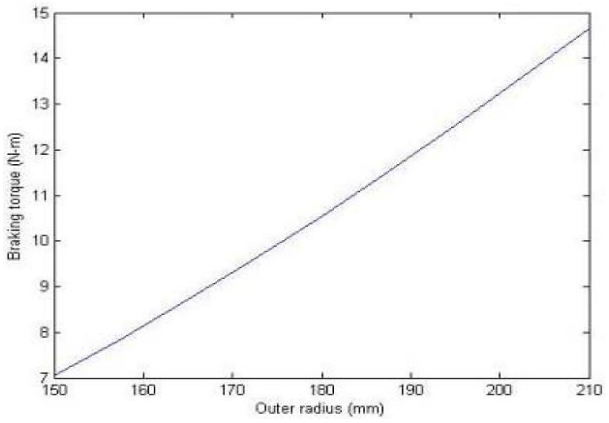

Fig.6 Braking torque of MR brake using conventional disc

It shows that the braking torque is limited to 14.5 Nm. To enhance the braking torque, analyses have been performed using waveform boundary disc.

Considering the values of τ_o (= 56 kPa), h (= 1 mm), h_o (= 8 mm), R_1 (= 50 mm) and ω (= 30 rad/s), the braking torque of MR brake has been estimated using Eq. (21). Figure 7 and Figure 8 show the braking torque at t = 10 mm and at t = 8 mm.

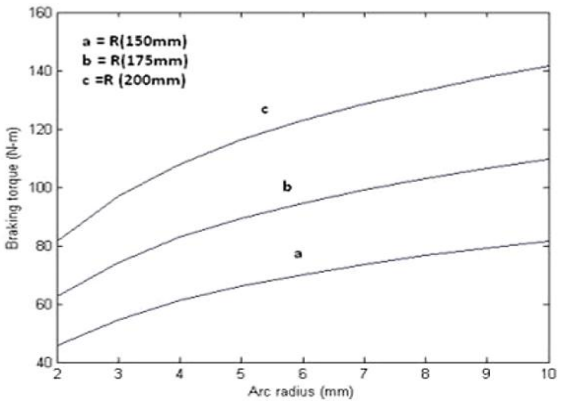

Fig.7 Braking torque with respect to focal distance of parabolic profile

Figure 7 and Figure 8 show that the braking torque is increasing as the radius of the waveform and thickness of the disc is increasing. Figure 9 and Figure 10 show the braking torque of MR brake for same thickness (t = 8 mm) for parabolic and circular profile respectively. From the Figure 9 and Figure 10 it is clear that braking torque achieved with the parabolic profile is larger than the circular profile.

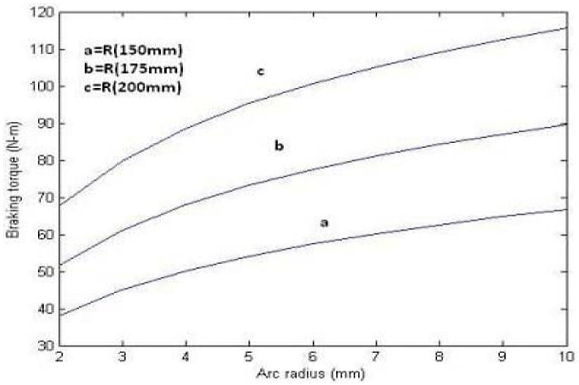

Fig.8 Braking torque with respect to focal distance of parabolic profile

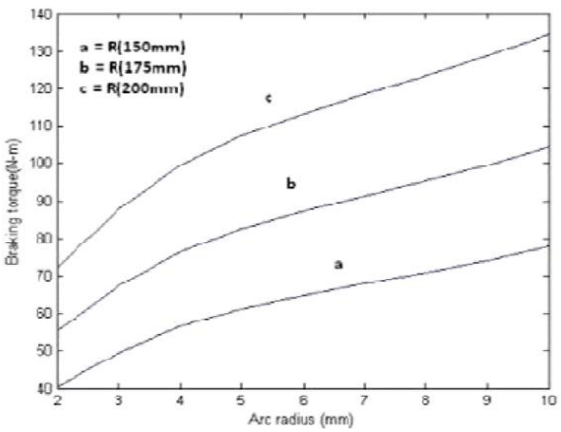

Fig.9 Braking torque with respect to arc radius of parabolic profile

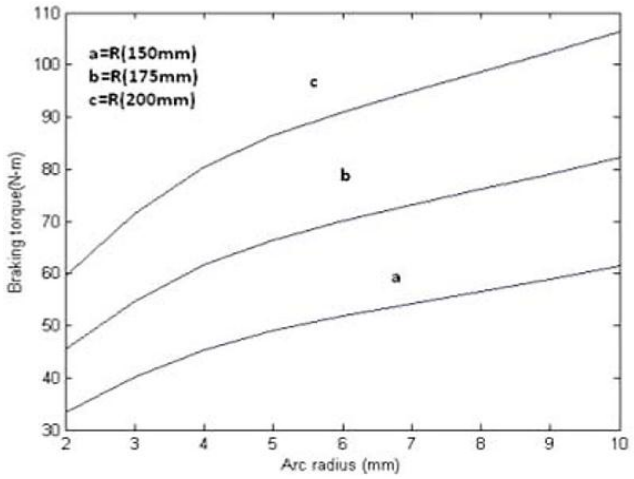

Fig.10 Braking torque with respect to arc radius for circular profile

Figure 11 and Figure 12 show the braking torque of MR brake at various MR gaps for parabolic profile and circular profile respectively.

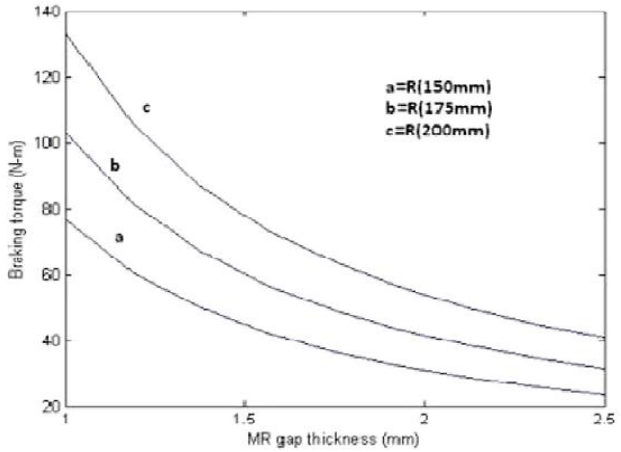

Fig.11 Braking torque with respect to MR film thickness for parabolic profile

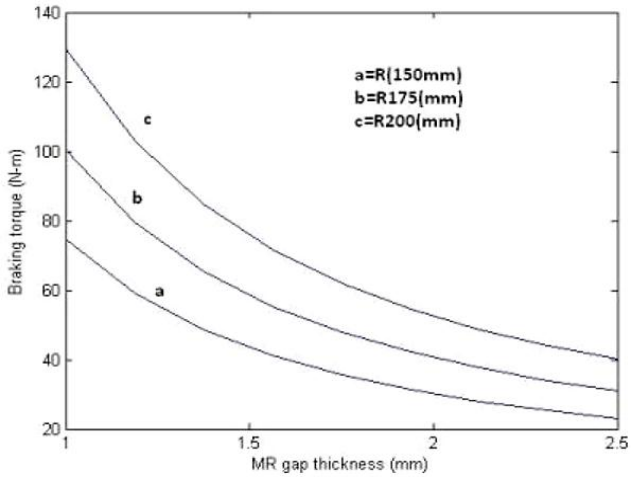

Fig.12 Braking torque with respect to MR film thickness for circular profile

From Figure 11 and Figure 12, it is clear that the braking torque is decreasing as the film thickness is increasing because due to increase in the MR gap thickness the magnetic field in the gap become weaker. Figure 13 shows the braking torque of MR brake at various input currents.

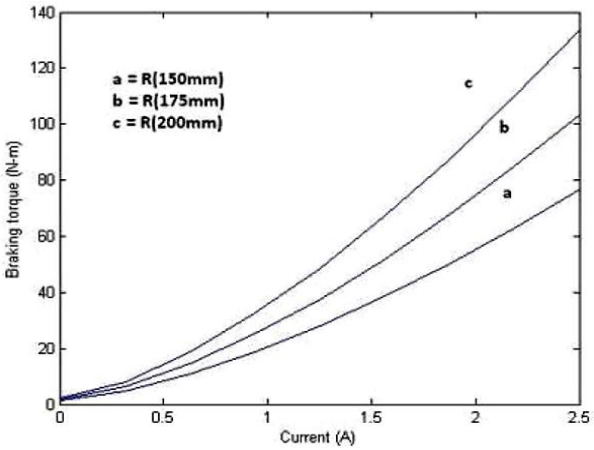

Fig.13 Braking torque with respect to applied current

From Figure 13 it is clear that braking torque is increasing as the applied current is increasing at the fixed no of coil due to the increase in the shear stress in the influence of magnetic field. At the zero value of the current there is some value of the resisting torque due to the no field viscosity of the MR fluid. The details drawing and model of fabricated MR brake with wave form boundary is shown in Figure 14.

Fig.14 Disc with waveform boundary

Conclusions

This research work has discussed the effect of different parameters on the braking torque of MR brake. The following conclusions can be made from the present research work.

- Braking torque is increasing as the radius of the waveform and thickness of the disc is increasing.
- Braking torque achieved with the parabolic profile is larger than the circular profile.

- Braking torque is decreasing as the film thickness increases.
- With increase in applied current, there is an increase in braking torque.

References

C.Sarkar, H.Hirani, (2013), Theoretical and experimental studies on a magnetorheological brake operating under compression plus shear mode, *Smart Materials and Structures*, 22, art. no. 115032.

C.Sarkar, H.Hirani, (2013), Synthesis and characterization of antifriction magnetorheological fluids for brake, *Defence Science Journal*, 63, pp. 408-412.

C.Sarkar, H. Hirani, (2013), Design of a squeeze film magnetorheological brake considering compression enhanced shear yield stress of magnetorheologicalfluid, *Journal of Physics: Conference Series*, 412, 012045.

C. Sarkar, H. Hirani, (2015), Transient thermoelastic analysis of disk brake, International Journal of Current Engineering and Technology, 5, pp. 413-418.

C. Sarkar, H. Hirani, (2015), Magnetorheological smart automotive engine mount, International Journal of Current Engineering and Technology, 5, pp. 419-428.

C. Sarkar, H. Hirani, (2015), Finite element analysis of magnetorheological brake using ANSYS, International Journal of Current Engineering and Technology, (accepted).

C. Sarkar, H. Hirani, (2015), Synthesis and characterization of nano-copper-powder based magnetorheological fluids for brake, International Journal of Scientific Engineering and Technology, 4, pp. 76-82.

C.Sarkar, H.Hirani, (2015), Effect of particle size on shear stress of magnetorheological fluids, *Smart Science,* (in press).

C. Sarkar, H. Hirani, (2015), Development of magnetorheological brake with slotted disc, *Proc. IMechE, Part D: Journal of Automobile Engineering*, (in press).

H.Hirani, C. S. Manjunatha, (2007), Performance evaluation of magnetorheological fluid variable valve, *Proc. of the Institution of Mechanical Engineers, Part D, Journal of Automobile Engineering*, 221, pp. 83-93.

J. M. Ginder, L. C. Davis,(1994), Shear Stresses in Magnetorheological fluids: Role of Magnetic Saturation, Applied Physics Letters, 65, pp. 3410-3412

T. H. Nam and K.K. Ahn, (2009), A new structure of a magnetorheologicalbrake with the waveform boundary of arotary disk", Smart Mater.Struct.18, 15029

S. Gupta, H. Hirani, (2011), Optimization of magnetorheological brake, *ASME/STLE 2011 International Joint Tribology Conference*, pp 405-406.

V.K.Sukhwani, V.Lakshmi, H. Hirani, (2006), Performance evaluation of MR brake: an experimental study, *Indian Journal of Tribology*, pp. 67-52.

V.K.Sukhwani,H.Hirani,T.Singh,(2007), Synthesis of magnetorheologicalgrease,*Greasetech India*.

V.K.Sukhwani, H.Hirani, (2007), Synthesis and characterization of low cost magnetorheological (MR) fluids, *The 14th International Symposium on: Smart Structures and Materials & Nondestructive Evaluation and Health Monitoring*, 65262R-65262R-12.

V.K.Sukhwani, H.Hirani, (2008), A comparative study of magnetorheological-fluid-brake and magnetorheological-grease-brake, *Tribology Online*, 3, pp. 31-35.

V.K.Sukhwani, H.Hirani, T.Singh, (2008), Synthesis and performance evaluation of MR grease, *NLGI Spokesman*,71.

V.K.Sukhwani, H. Hirani, (2008), Design, development and performance evaluation of high speed MR brake, *Proc. Institute Mech. Engineers., Part L, Journal of Materials: Design and Applications*, 222,pp.73-82.

V.K.Sukhwani, H.Hirani, T. Singh, (2009), Performance evaluation of a magnetorheological grease brake, *Greasetech India*, 9,pp. 5-11.